JOURNAL OF APPLIED ELECTROCHEMISTRY 19 (1989) 729–735

Analysis of molten industrial silicates by electrochemical techniques

B. LAFAGE, P. TAXIL

Laboratoire de Chimie-Physique et d'Electrochimie, UA CNRS 192, Université Paul-Sabatier, 118, route de Narbonne 31062 Toulouse Cedex, France

Received 12 June 1988; revised 21 February 1989

Fused silicate glass is investigated in this work by electrochemical techniques, using platinum as a convenient material for reference, working and auxiliary electrodes. Cyclic voltammetry and chronopotentiometry are carried out whenever possible, mainly in the case of colourless glass. For more complex systems, square-wave voltammetry is preferred since its mathematical treatment allows the waves of interfering electrochemical reactions to be separated. So, the oxidation of oxygen anions, the reduction of sodium ions and Fe oxides are studied in some detail and the feasibility of the attempted techniques in the fused glass are discussed.

1. Introduction: electrochemistry in glass

Molten industrial glass is an ionic liquid in which the solvent is the ternary system SiO_2–Na_2O–CaO in the respective proportions of about 74: 13 : 12 mass per cent. The batch composition also includes approximately 1% of a series of other constituents which intervene during the fusion process.

The fusion of polymerized silica is promoted by the reaction with O^{2-} ions delivered by sodium and calcium oxide dissociation, according to the following equilibrium [1]:

$$\equiv Si\text{–}O\text{–}Si\equiv + O^{2-} \rightleftharpoons 2\,(\equiv Si\text{–}O)^{-} \qquad (1)$$

The O^{2-} ion content characterizes the acidity of the media, as in the Lux concept [2]. The calculations of the acidity constant of various glasses by Toop and Samis [3] and Holmquist [4] have established the close dependence of O^{2-} ion content on the nature and the composition of the fusing oxides. Furthermore, it is shown to be sensitive to the partial pressure of oxygen above the glass and the presence of ionic constituents in the melt, as shown in the following equation, suggested by Paul and Douglas [5]:

$$M^{p+} + \frac{q}{4}\,O_2 \rightleftharpoons M^{(p+q)+} + \frac{q}{2}\,O^{2-} \qquad (2)$$

in which M is an electroactive species such as iron, chromium or sulfur compounds. Iron and chromium are used to give specific colourations to the final products. The addition of sulphur to the batch mixture, either as sodium sulphate or sulphide or as a mixture of both, tends to accelerate the fusing and refining process [6].

Ionic interaction within the fused glass leads to a new oxidation state of each electroactive species and, afterwards, may influence the further thermic, optic and mechanical properties of the material. To date, chemical analyses of glass have always been performed on the cold material by means of physical and chemical techniques including those involving electrochemistry but it can be assumed that some change of the oxidation state of the elements can occur during the cooling step in the atmosphere and the preparation of the sample. Thus, the analysis 'in situ' of the fused melt would be preferable and electrochemical techniques have been suggested as particularly advantageous.

So, using cyclic voltammetry, Takahashi and Miura had previously determined redox potentials of various systems and diffusion coefficients of ions in molten industrial glasses [7]. More recently, Claes and Glibert demonstrated that the width of the voltammetric waves due to the high temperatures involved in these media, was too great to make this technique sensitive enough for quantitative analysis [8]. They suggested the use of impulse techniques which lead to better defined peaks and they applied the differential pulse voltammetry (DPV) to the titration of cobalt in soda lime silicates.

Likewise, Freude and Russel demonstrated the superiority of another impulse technique, square-wave voltammetry (SWV) over the cyclic voltammetry for the investigation of the Fe^{III}/Fe^{II}, As^{V}/As^{III} and As^{III}/As^{0} systems in molten glasses [9]. In particular, they emphasized the sensitivity of SWV which allows low concentrations of ferric ions to be detected, but they did not give any information on the further reduction of ferrous ions.

This paper describes electrochemical studies in industrial glass melts at 1100° C and confirms and completes some of the preceding conclusions. So, in the case of the iron system, the mechanism of the overall reduction of Fe^{III} will be proposed, by means of a specific treatment of the square-wave voltammogram related to the reduction of this species.

0021-891X/89 $03.00 + .12

2. Experimental details

2.1. *The electrolytic cell*

This consisted of a cylindrical can of Inconel capped by a set of stainless steel, water-cooled flanges. The upper flange was a cover provided with electrode passages. Viton 'O-rings', between the flanges and cylindrical Teflon gaskets in the passages allowed the set-up to be hermetically sealed and, then, to be placed under controlled atmosphere when necessary.

2.2. *Electrodes*

The working and auxiliary electrodes were, respectively, a platinum wire (diameter: 2 mm; immersed length: 1 cm) and a platinum rod with a large surface area. A platinum wire, directly immersed in the bath, was used as reference electrode. The potential of this electrode is associated to the reversible system O_2/O^{2-}. As it is sensitive to both the acidity of the melt and the partial pressure of oxygen (pO_2) above the bath, some shift of the potential scale may occur when these parameters are changed. Desportes and Darcy's electrode, in which pO_2 is regulated inside a yttrium-doped zirconia sheath [10], does not correct the variation of $[O^{2-}]$. Moreover, this electrode has a too short lifetime. So, platinum wire was preferred, since the correction of the potentials can be made by using the solvent reduction wave as another mark.

2.3. *Electrolytic bath*

The experimental melt was made up of an oxide mixture, provided by a glass-making factory, previously fused, refined and analyzed, after cooling, by X-ray fluorescence and spectroscopy. Table 1 gives the composition of the mixtures mentioned in this paper. The melt was placed in an alumina crucible inside the cell. A mullite liner surrounded the crucible in order to screen the melt from the corrosion products of the heated Inconel parts of the cell.

2.4. *Techniques of analysis*

Conventional techniques (cyclic voltammetry, chronopotentiometry) are available for investigation of simple systems, where no interference between the electrochemical reactions occurs otherwise. SWV was preferred in this work. Here, the waveform resulted from the sum of synchronized square-wave and staircase potential (E). Direct and reverse polarization alternated over each period with the same signal height (ΔE). The differential current (δi) was measured between the two successive steps in such a manner that only the Faradaic component was taken into account. So, for each electrochemical reaction, superactivation of the electrode was promoted and reached a maximum value when the staircase potential was $E_{1/2} - \Delta E$, where $E_{1/2}$ is the half-wave potential. This technique was fully developed, in the case of reversible systems, by Osteryoung *et al.* [11–13]. The mathematical model, leading to the theoretical expression of δi, applied in this work, is detailed in Ref. [14].

Table 1. Composition of glass melts used in this work (mass per cent)

Constituents	*A*	*B*	*C*	*D*	*E*
SiO_2	73.50	72.08	71.26	71.84	72.49
Na_2O	13.00	14.92	13.01	15.85	13.88
CaO	12.00	10.86	11.76	10.33	10.44
K_2O	–	0.23	0.41	0.03	0.05
Al_2O_3	1.50	1.74	1.72	1.75	2.55
TiO_2	–	0.02	0.05	0.03	0.06
SO_3	–	0.02	0.16	0.02	–
Fe_2O_3	–	0.03	0.33	0.05	0.35
Cr_2O_3	–	–	0.25	–	–

The voltammogram of each reaction, $\delta i = f(E)$, has a Gaussian shape around a peak at a potential $E_p = E_{1/2} - \Delta E$ with δi_p proportional to the content of the electroactive species.

The width of the peak at half-height ($W_{1/2}$) is given by the following equation:

$$W_{1/2} = 3.52RT/nF \tag{3}$$

as long as $\Delta E < 0.5RT/nF$.

In the case of a multicomponent system, with interfering waves, the resulting differential current is formally expressed as follows:

$$\delta i(E) = \sum_{j=1}^{N} \delta i_p^j f_j(E) \tag{4}$$

N is the number of components of the system, $f_{(j)}(E)$ is a function depending, in particular, on the number of electrons and the equilibrium potential of each of them. If these parameters are not known with accuracy, trial and error fitting of values has to be made before coincidence between the model voltammogram and the experimental data is obtained. So, the separation of the wave components can be achieved.

In this work, SWV experiments required the use of a microcomputer connected to an EG&G potentiostat (model PAR 273).

3. Results and discussion

3.1. *Experiments in soda-lime silicates without additives*

The cyclic voltammogram of a colourless glass melt (an example is shown in Fig. 1 for a glass melt denoted B, and the composition of which is given in Table 1), allows the electroactive range of these media, which is extended between -0.9 V and $+0.1$ V versus the platinum reference, to be defined The oxidation and reduction parts of this curve will be considered in some detail.

3.1.1. Anodic part. The oxidation of O^{2-} ions leads to oxygen evolution, following an apparent two-phased

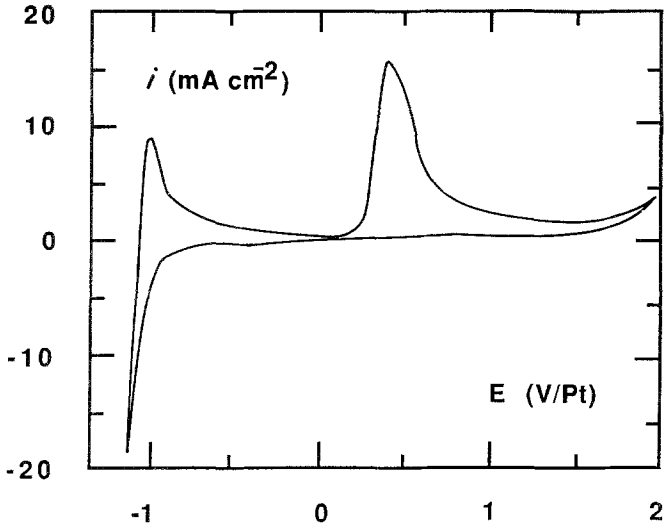

Fig. 1. Cyclic voltammogram of a colourless glass melt (B of Table 1; temperature: 1150°C; atmosphere: air; scanning rate of potentials: 1 V min^{-1}).

mechanism. The first step is marked by a peak-shaped curve at lower overpotentials on the voltammogram, associated to the formation of a platinum-oxygen compound and followed by a (gas release) step.

This compound may either be a platinum oxide as suggested by Higgins based on chronopotentiometric measurements [15, 16], or an adsorbed species according to Moortgate-Hasthorpe's impedance measurements [17]. This second assumption seems to be confirmed by our measurements of double layer capacitance and the resistance of the platinum interface.

Here, the technique consists of superimposing pulses of potential to the polarized electrode. As the electrode interface is similar to a resistance and a capacitance placed in parallel, the charging current of the capacitance is given by the following equation [18]:

$$i = \frac{E \exp(-t/R_s C_d)}{R_s} \qquad (5)$$

R_s is the interface resistance of the electrode and C_d the double layer capacitance. At the beginning of the pulse (for less than one millisecond), the Faradaic current can be ignored and the current–time evolution is assumed to follow Equation 5. Thus, both values of R_s and C_d may be calculated by measuring the slope and the origin intercept of the straight line $\log i = f(t)$.

Figure 2 shows that the highest values of C_d are obtained in the potential range where the peak is observed on the voltammogram. This result is in agreement with the measurements of C_d by Moortgate-Hasthorpe *et al.*; the decrease of C_d at more oxidizing potentials (above 0.35 V vs platinum) means that a new step in the chemisorption phenomenon could intervene. It is relevant to point out that a simultaneous increase of the resistance of the interface electrode and a sharp decay of the current on the voltammogram are produced by higher anodic overpotentials. They may be correlated with both the formation of inactive chemisorbed species and bubbles of oxygen gas released at the surface of the electrode. In fact, bubbles were noticed within the glass remaining on the polarized electrode when it was quickly withdrawn from the cell.

The formation of the oxycompound may also be correlated with the plateau observed on the chronopotentiogram of Fig. 3. If τ is the transition time, the product $i\tau^{1/2}$ is found to be a constant and the Sand equation is seen to be followed in Fig. 4. These results confirm Ruch's chronopotentiometric studies in molten SiO_2–Na_2O mixtures [18]. This author has also stated that the anodic reaction is controlled by the interdiffusion of sodium cations and oxygen anions at the platinum interface, promoted by the discharge of oxygen anions.

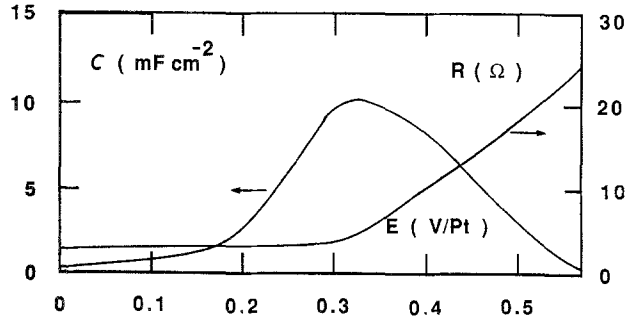

Fig. 2. Variation of the double layer capacitance and the resistance of the solution at the electrode interface in the anodic range of potential.

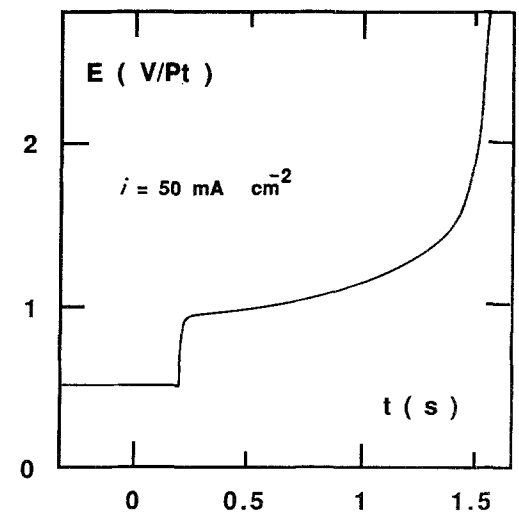

Fig. 3. Oxidation of O^{2-} ions by chronopotentiometry (glass melt: *A*; temperature: 1150°C; atmosphere: air).

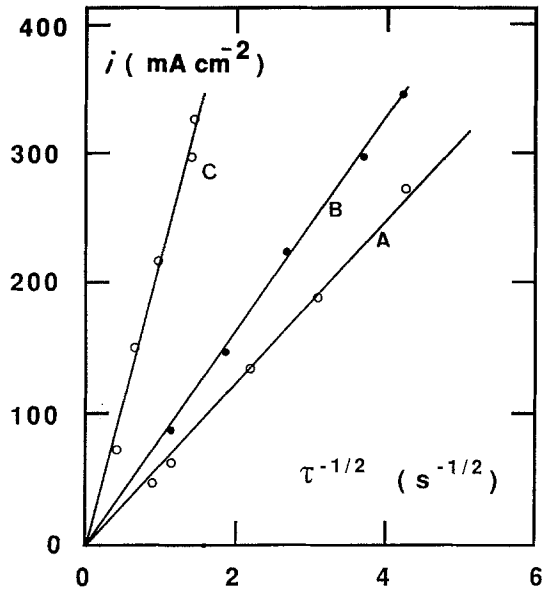

Fig. 4. Verification of the SAND equation for the anodic chronopotentiograms of glass melts A, B and C (temperature: 1100° C; atmosphere: air).

Moreover it is seen in Fig. 4, that the slope of the straight lines is affected by the composition of the glass melt (see Table 1) for the three samples represented. If we consider the expression for the slope:

$$i\tau^{1/2} = \frac{\pi^{1/2} n F C_0 D^{1/2}}{2} \qquad (6)$$

where C_0 is the concentration of oxygen ions and D is the interdiffusion coefficient of these ions, which is independent of C_0 according to Ruch, it may be expected, according to Table 1, that the basicity of these melts increases from A through B to C as suggested by the fusing oxide content.

Therefore, according to these results, the measurement of the product $i\tau^{1/2}$ could be a convenient index of the basicity of these media.

3.1.2. Cathodic part. Only one wave reduction is exhibited on the voltammogram of Fig. 1, whereas a shoulder observed in this wave on the square-wave voltammogram of Fig. 5 seems to indicate that two successive steps intervene. The separation of the two waves can be achieved by applying the technique mentioned above as shown in Fig. 6. The good agreement between the calculated model and the experimental curve is noticed in this figure. So, we can assume that a first step reduction, marked by a peak at about -1 V intervenes at potentials less than -0.7 V vs platinum. The number of electrons, involved in this reaction, deduced from the width of the peak at half height of it ($W_{1/2}$) (see Equation 3), is found to be near unity. Afterwards, a second reduction step begins at a potential less than -0.95 V.

Taking into account both the thermodynamic calculations, which allow us to state that the dissociation energy of sodium oxide is the lowest of the three solvent components [17] and the number of electrons found as above, the first step corresponds to sodium ion reduction. Nevertheless, this assumption can be criticized since the mathematical treatment of SWV is valid only in the case of diffusion processes, whereas the flow of Na^+ in glass media may be considered to be controlled by migration [19]. Thus further complementary experiments are necessary to confirm these hypotheses.

3.2. *Experiments with a glass melt containing iron*

3.2.1. Cyclic voltammetry and semi-integration. The cathodic part of a cyclic voltammogram performed with a glass melt including Fe_2O_3 in its batch composition (*E* in Table 1) exhibits only one reduction wave close to the solvent wave (Fig. 7), whereas both valences II and III of iron are supposed to be present in the fused mixture. The interval between reduction and reoxidation peaks is approximately 140 mV. So, this system can be considered as reversible. Semi-

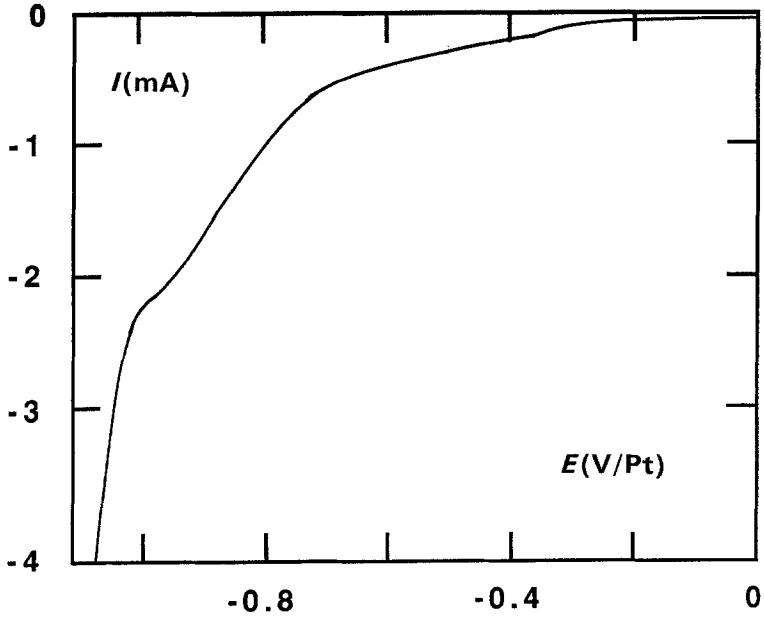

Fig. 5. Cathodic square-wave voltammogram of a colourless glass (melt D; temperature: 1050° C).

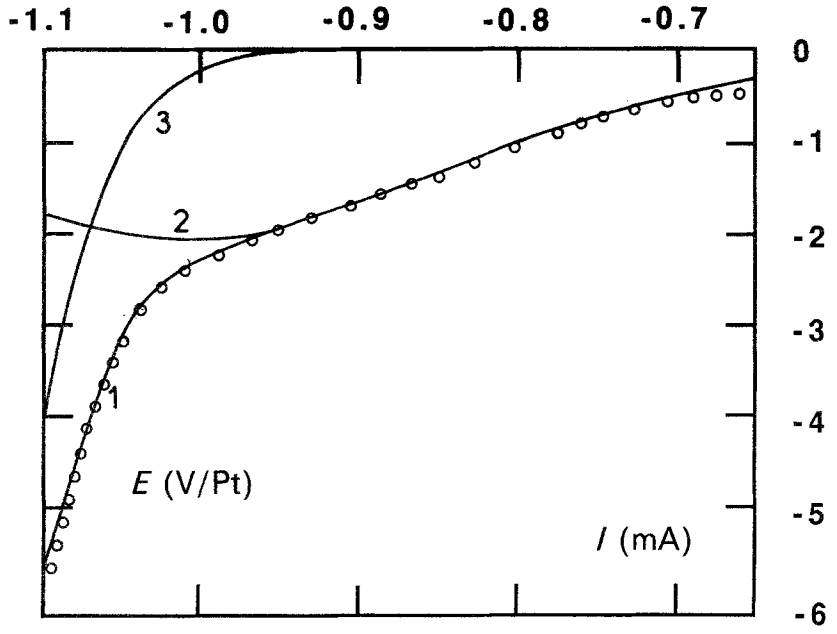

Fig. 6. Breaking up of the square-wave voltammogram of Fig. 6. (1) Experimental curve; (2) reduction of sodium ions; (3) reduction of silicate ions; ooo calculated resulting curve.

integration of the current leads to the following voltammogram equation, only valid in the case of reversible systems [20]:

$$E = E_{1/2} + \frac{RT}{nF} \ln \frac{I_l - I_t}{I_l} \qquad (7)$$

I_t is the semi-integrated current:

$$I_t = \frac{1}{\pi^{1/2}} \int_0^t \frac{i(u)}{t - u} \, du \qquad (8)$$

I_l is the limiting value of I_t, and is a linear function of the electroactive species content. Equation 8 allows the number of electrons to be calculated.

After correction of the residual current (measured with a colourless glass mixture), the iron reduction wave exhibits a well-defined peak (Fig. 8). Then, semi-integration results are plotted in Fig. 9: curve (1) is the experimental graph I_t versus E; I_l is the current peak. Equation 8 is followed on curve (2); n is calculated from the slope of the straight line and is found to be on average, 1.78, which is clearly an intermediate value between the number of electrons involved in the successive steps Fe^{III}–Fe^{II} and Fe^{II}–Fe^{0}. Thus, the voltammetric technique only takes into account the resultant reduction wave for the two successive steps Fe^{III}–Fe^{II} and Fe^{II}–Fe^{0}.

This situation has to be correlated with the theoretical e.m.f. of the galvanic cells associated with the following reactions:

$$2FeO + 3/2O_2 \rightleftharpoons Fe_2O_3 \qquad (9)$$

$$Fe + 1/2O_2 \rightleftharpoons FeO \qquad (10)$$

According to the thermodynamic data, previously reported by Gaur and Sethi [21], the E_0 values of these reactions (respectively −656 and −888 mV with respect to the normal oxygen electrode) are relatively close together, possibly explaining the interference of the two successive waves. This is confirmed by SWV.

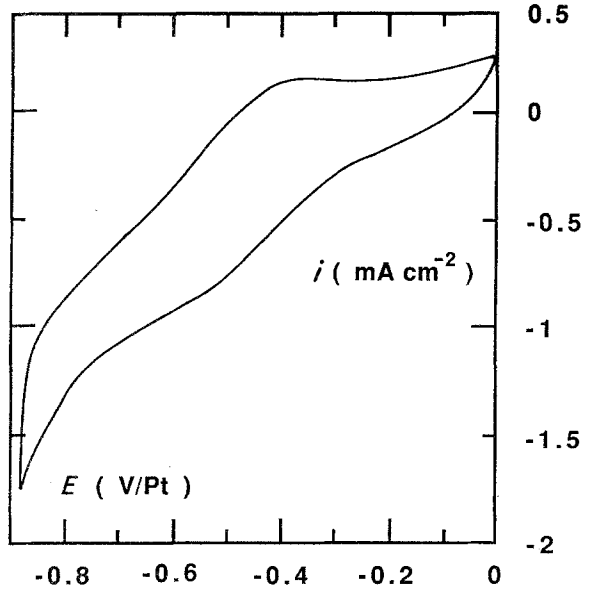

Fig. 7. Cathodic part of a cyclic voltammogram performed on a glass melt containing iron oxides (glass melt E; temperature: 1100°C; atmosphere: air; scanning rate: 1 V/min).

3.2.2. Square-wave voltammetry. Figure 10 shows the cathodic part of the square-wave voltammogram of the glass melt E (curve 1). Each component of this voltammogram can be defined, taking into account the following assumptions:

(1) In the potential range examined, only the first step of solvent reduction is to be taken into account (see Fig. 6).

(2) The reaction $Fe^{III} + e^- \leftrightarrows Fe^{II}$ begins at a more anodic potential than $Fe^{II} + 2e^- \rightleftarrows Fe$, but the associated peaks of differential current are very close together.

The resolution of the system of Equation 4 requires trial and error to determine both the peak differential current and potential of each reaction. It leads to the separation of the waves, shown in Fig. 10, which is validated by the agreement between the attempted model and the experimental curve. So,

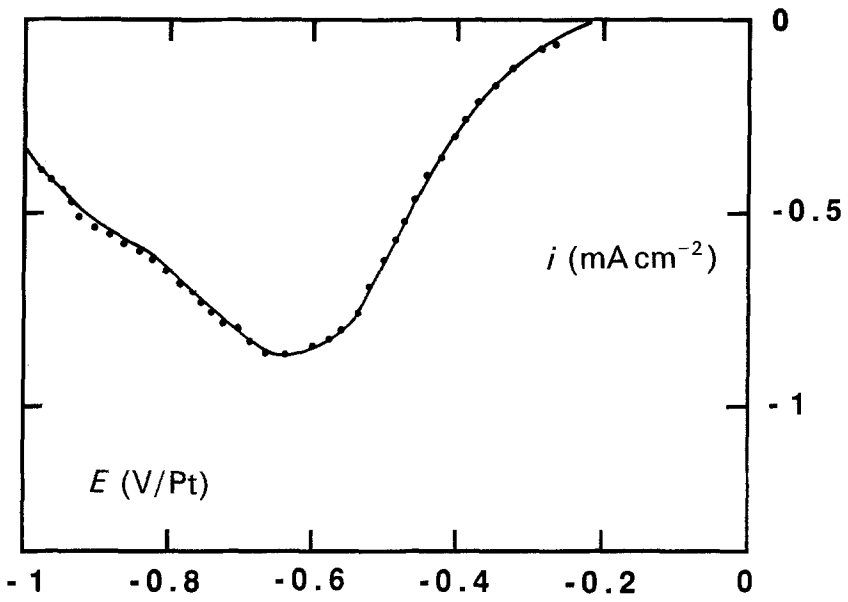

Fig. 8. Voltammogram of the iron reduction wave after correction of the solvent wave (glass melt: E; temperature: 1100° C; atmosphere: air; scanning rate: 1 V/min).

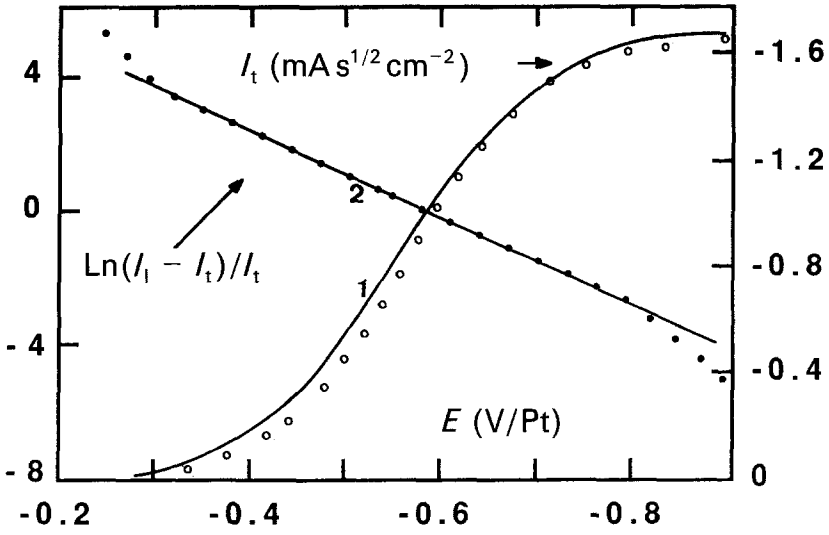

Fig. 9. Semi-integration of the voltammogram of Fig. 8. (1) Experimental variation $I_t = f(E)$; (2) verification of Equation 7; ooo calculated variation $I = f(E)$.

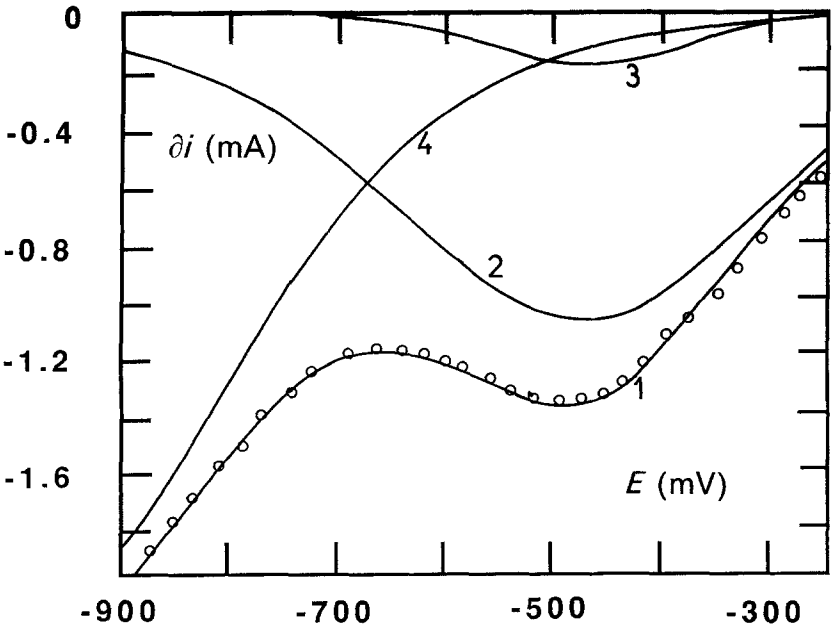

Fig. 10. Cathodic square-wave voltammetry of the glass melt E (temperature: 1100°C; atmosphere: air). (1) Experimental curve; (2) reduction of Fe(III); (3) reduction of Fe(II); (4) reduction of sodium; ooo calculated resulting voltammogram.

Table 2. Evolution of the ∂i_p related to the Fe^{III} reduction and Fe^{II} reduction of Fig. 10, after placing the melt under an argon atmosphere at 1100° C

Time (hours)	*Fe^{III} reduction ∂i_{p1} (mA)*	*Fe^{II} reduction di_{p2} (mA)*	$di_{p1}/\partial i_{p2}$
0	1.047	0.162	6.46
3	0.812	0.352	2.53
9	0.743	0.366	2.03
16	0.665	0.384	1.73
39	0.530	0.395	1.34

according to this figure, we have:

$$Fe^{III} + e^- \leftrightarrows Fe^{II} \text{ (curve 3)} \quad E_{1/2} = -0.451\,V \tag{11}$$

$$Fe^{II} + e^- \rightleftarrows Fe^0 \text{ (curve 4)} \quad E_{1/2} = -0.443\,V \tag{12}$$

So, as was assumed above, the quite different E_0 values of these reactions are not in disagreement with the closeness of the corresponding waves, since the $E_{1/2}$ of each of them are similar.

A further experiment confirmed the preceding mechanism and emphasized the sensitivity of the method: the natural atmosphere above the glass melt was replaced by an argon gas atmosphere for several days and successive SWV experiments were performed during the period.

The lack of oxygen above the melt enhances the Fe^{II}/Fe^{III} ratio since the reduction of Fe^{III} by O^{2-}, according to the general Equation 2, is made thermodynamically possible by the shift of the redox potential of the O_2/O^{2-} system towards more cathodic potentials than that of the Fe^{III}/Fe^{II} system, due to the low partial pressure of oxygen in commercial argon gas. It is to be noticed that Shreiber *et al.* have observed this phenomenon and correlated the redox state of iron with the fugacity of oxygen above the bath [21].

Table 2 exhibits a simultaneous increase of the Fe^{II} peak and decrease of the Fe^{III} peak during the period mentioned above; so, the preceding mechanism of the reduction of ferric ions in glass is confirmed.

4. Concluding remarks

The analysis of molten glass by means of electrochemical techniques has the advantage of relative ease but some difficulties remain. Some of these were overcome in this work.

The electroactive field is particularly narrow with a platinum working electrode. So, the interference of the electrochemical reactions is a real and unavoidable problem which is made more critical by the broadening of the waves, caused by high temperatures. Nevertheless, pulse techniques, such as SWV, have proved to be valid for the separation of the waves. A typical example of feasibility was presented for the Fe^{III}/Fe^{II} system. Now, other systems, including sulphur and chromium are being investigated. So, a quite complete analysis of the main electroactive species (including the O^{2-} ions) within the fused industrial glass will soon be achieved.

For a precise quantitative analysis, the calibration of the peaks requires previous titration of the electroactive species in each oxidation state, preferably *in situ*.

Acknowledgements

The authors are grateful to the society BSN Emballage and, in particular, MM. Pajean, Perez, Burnaz and Floriot for financial support and technical assistance.

References

[1] H. Flood and T. Forland, *Acta Chem. Scandinavica* **1** (1947) 592.
[2] H. Lux, *Z. Elektrochem.* **45** (1939) 303.
[3] G. W. Toop and C. S. Samis, *Trans. Metall. Soc. A.I.M.E.*, **224** (1962) 878.
[4] S. Holmquist, *J. Amer. Ceram. Soc.* **49** (1966) 467.
[5] A. Paul and R. W. Douglas, *Phys. Chem. Glasses* **7** (1966) 1.
[6] M. Pierret, *Silicates Industriels* **2** (1976) 39.
[7] K. Takayashi and Y. Miura, *J. Non-cryst. Solids* **38–39** (1980) 527.
[8] P. Claes and J. Glibert, *Rivista della Sper. vetro* **5** (1985) 229.
[9] E Freude and C. Russel, *Glastech. Ber.* **60** (1987) 202.
[10] J. Besson, C. Desportes and M. Darcy, *C. R. Acad. Sci.* **251** (1960) 630.
[11] J. H. Christie, J. A. Turner and R. A. Osteryoung, *Anal. Chem.* **4** (1977) 1899.
[12] J. J. Dea, J. Osteryoung and R. A. Osteryoung, *ibid.* **53** (1981) 695.
[13] J. Osteryoung and R. A. Osteryoung, *ibid.* **57** (1985) 101.
[14] L. Ramaley and M. S. Krause, *ibid.* **41** (1969) 1363.
[15] J. K. Higgins, *Glass Technology* **21** (1980) 145.
[16] J. K. Higgins, *ibid.* **23** (1982) 90.
[17] M. Moortgate-Hasthorpe, H. Van Der Poorten and A. Blave, *Silicates Industriels* **11** (1976) 463.
[18] L. M. Ruch, Thesis, Univ. Pennsylvania, USA (1977).
[19] C. Thirion, Thesis, Univ. Grenoble, France (1980).
[20] A. J. Bard and L. R. Faulkner, 'Electrochemical Methods, Fundamental Applications', J. Wiley and Son Inc Publisher, New York (1980).
[21] H. C. Gaur and R. S. Sethi, *Ind. J. Chem.* **5** (1967) 485.
[22] H. D. Schreiber, H. V. Lauer Jr and T. Thanyasiri, *J. Non-cryst. Solids* **38–39** (1980) 785.